HI Absorption in High-Z SDSS-III/BOSS Type-2 Quasars: Disentangling the UV Interpretation

Claire Cook*
Department of Physics and Astronomy,
University of Kansas, Lawrence, KS, 66045, USA

(Dated: August 22, 2021)

Probing the interplay between AGN feedback and host galaxy evolution is a hot topic in current astronomy research. HI-absorption traces the presence of cold, neutral gas in galaxies and previous works find progressively fewer detections of HI in quasar sources after redshifts of $z > 0.5$, possibly due to HI photoionization in quasars with $L_{UV} > 10^{23} W/Hz$. However, these works are lacking in high-z, Type-2 sources. This project takes 18 such quasars identified by SDSS-III/BOSS, allowing further exploration of the connection between UV luminosity and HI photoionization. Two potential detections of HI absorption requiring follow-up are reported.

I. INTRODUCTION

The accretion process of active galactic nuclei, or AGN, releases incredible amounts of energy into the surrounding environment, naturally having an impact on the host galaxy and how that host then evolves. However, this interplay between the AGN and host galaxy is complicated and not yet well-understood.

The 1420-MHz HI line is one tool that can be used to explore this relationship. Because this line in absorption traces the presence of cold, neutral gas in the host galaxy, whether or not HI is detected may indicate the effects of quasar output on the galactic medium.

Previous works suggest the following: (i) that HI can be photoionized by the quasar's energy output, unless it is shielded by dust or sufficiently-high column densities, (ii) that this photoionization can be related to the source's UV luminosity, and after a $L_{UV} \gtrsim 10^{23} W/Hz$, it is expected that all HI in a galaxy should be photoionized, and (iii) that there are fewer HI detections in sources with redshifts of $z > 0.5$, implying a redshift dependence for this effect [1, 2]. However, these works have some observational limitations. Sources with UV luminosities of $L_{UV} > 10^{23} W/Hz$ dominate surveys and there is a scarcity of Type-2 and high-z sources. This begs the question of whether the decreasing HI detection fraction is observed due to the observation of more powerful Type I sources, rather than the photoionization interpretation.

When Type I quasars are observed, by the unified model, the AGN is being viewed directly and without obscuration from the dusty torus. Type II quasars, by contrast, are being viewed through the dusty torus. Less detected absorption may naturally be expected when more Type I objects are viewed than Type II.

The aim of this project is to take undersampled objects to shed further light on the effects of quasar activity on the host galaxy's gas content. By expanding the sample and finding upper limits on HI content for our Type II sources, we hope to disentangle whether the lack of HI detections at higher z's and UV luminosities is due to photoionization from quasar output, or if there's a difference in the amount of HI detections when looking at Type I versus Type II sources.

II. THE SAMPLE, OBSERVATIONS AND ANALYSIS

This project's sample consisted of 18 Type II quasars with redshifts of $0.55 < z < 1.0$ and varying UV luminosities. These sources have continuum flux densities > 100 mJy at the redshifted HI frequency, and sub-arcsec angular sizes from the FIRST catalog. The compactness of their sizes imply that most of the continuum emission is situated well within the host galaxies of these quasars. They were also selected to have HI lines in regions of the spectrum where less RFI was expected from existing monitoring data.

The data were taken in frequency-switching mode on the Green Bank Telescope, using the "PF1-800 MHz" receiver. Due to considerable RFI in the off-frequency state, bringing interference into the line region, data calibration, reduction, and analysis were performed utilizing the total power of the spectra. The data were converted from counts to Janskys, and bad data records were removed based on deviant RMS values. Orthogonal polarizations and the two frequency-switched states were averaged to reduce noise. Finally the reduced spectra were boxcar smoothed by 11 channels to a frequency resolution of 7.87 kHz.

CTA21, a galaxy with a known HI absorption feature, was used as an example and test source for all procedures. Prior work on CTA21's HI absorption [3] was used to evaluate consistency with current observations and thus determine the best method for baseline fitting and calibration. The absorption spectrum of CTA21 derived from the present GBT observation is presented in Fig 2. Baselines were fit to the spectra of our sample using approximately $\pm 600 km/s$ of the final, reduced spectra, with RFI and $\pm 50 km/s$ surrounding the expected

* Email: claire.cook@ku.edu

Source	z (uncertainty)	RMS [mJy]	# of scans	N(HI)
J0023+081	0.563796(32)	too much RFI	23	x
J0146-019	0.958851(55)	8.9205	3	9.76231E+19
J0910+243	0.905406(54)	8.1755	3	1.0264E+20
J0134+000	**0.574776(24)**	**1.9733**	**20**	**9.95777E+19**
J0903+041	0.720250	2.5967	34	2.77488E+20
J0922-007	0.575544(27)	1.289	33	1.42784E+20
J0935+438	0.593061(35)	3.4431	18	2.03743E+20
J0942+137	0.583475(44)	6.0228	3	2.23429E+19
J1004+318	0.563457(58)	5.9993	3	5.55486E+19
J1020+316	0.580207(30)	5.19685	3	7.30717E+19
J1110+482	**0.7412**	**3.34705**	**9**	**1.03233E+20**
J1138+502	0.718618(24)	6.21575	3	1.12581E+20
J1225+452	0.582571(32)	2.6335	10	9.2716E+19
J1312+501	0.564381(26)	5.8456	2	2.10703E+20
J1416+403	0.584519(43)	1.6567	19	1.41298E+20
J1603+146	0.981859(60)	4.5979	14	2.0778E+20
J1635+265	0.685801(27)	1.9893	19	1.47505E+20
J1654+315	0.553786(43)	too much RFI	4	x
CTA21	0.907	8.54749753	4	7.90E+20

FIG. 1. A table of all sources, their respective redshifts with uncertainty given in parentheses, RMS values of clean sections of baseline (if any), the number of scans taken of the source, and the calculated upper limits for HI column density. The highlighted lines represent the two potential detections.

line region omitted from the fitting process. The lowest polynomial that presented a good fit to the data was used for baseline subtraction.

RMS values were calculated on the baseline fits using the GBTIDL 'stats' function on sections of RFI-free baseline. Figure 3 shows that the rms noise after data reduction and baseline fitting is consistent with expectations.

Upper limits on HI column densities were found and catalogued for all sources using the equation,

$$N(HI) = 1.835 \times 10^{18} \frac{T_S \int \tau dV}{f_c} cm^{-2}, \quad (1)$$

where T_s is spin temperature (taken to be $100K$) and f_c is the covering fraction (taken to be 1). The upper limit on the numerator was found with:

$$\int \tau dV = \tau \Delta V, \quad (2)$$

where the value of ΔV was assumed from detections in the literature to be $33km/s$ and τ is equal to,

$$\tau = \frac{3RMS}{S_{HI}} \quad (3)$$

where S_{HI} is the continuum flux density of the source.

Sigma values were calculated for two potential detection (see Section III).

III. RESULTS

Figure 1 shows a summary of all 18 sources and their upper limit HI column densities, including 2 potential detections. The first potential detection, $J0134+000$, see Figure 5, was determined to be a 2σ detection, showing a dip feature below the baseline for approximately $\pm 50km/s$ surrounding the expected frequency of occurrence. While this may be an artifact resulting from the baseline fitting process, it also possibly constitutes a faint detection. The second potential detection, $J1110+482$, shown in Figure 6, was found to be a 2.4σ detection, showing a distinct dip near the line region of a recently updated redshift value. $J0134+000$ has a $log(L_{UV}[L_\odot]) = 22.83$ and $J1110+482$ has a $log(L_{UV}[L_\odot]) = 23.67$. Both of these sources are candidates for follow-up observations using the Green Bank Telescope to obtain increased sensitivity.

Figure 4 plots the upper limits of HI column density, N_{HI}/T_{spin} versus redshift to compare with the previous results of Curran and Duchesne 2018 [1]. It is found that all points are consistent with the upper limits of the previous work in this redshift range.

IV. CONCLUSIONS

18 Type-II quasar sources were analyzed in a search for detections of HI absorption; only 2 of these sources–$J0134+000$ and $J1110+482$–are candidates for potential detections and will require further observation to confirm detection.

The findings of this project are consistent with previous works [1, 3].

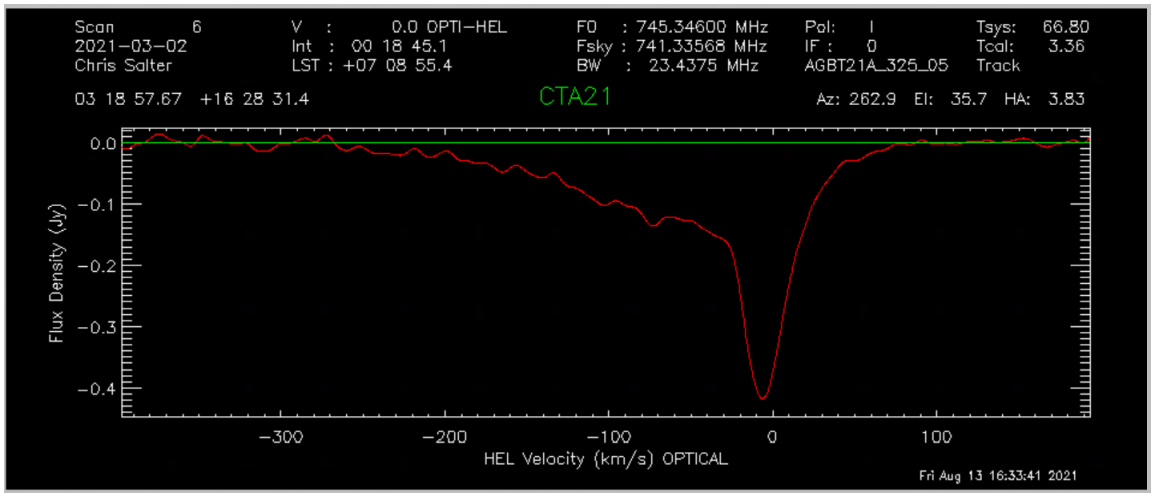

FIG. 2. The baseline-fitted spectrum for CTA21. The broadest, clean section of the reduced spectrum within $600km/s$ was taken, with a sizable area surrounding the line region omitted from the fitting process so as not to overfit the line's broad features as seen in previous work [3]. This process of taking about $600km/s$ of clean spectrum, while omitting an area of 50 km/s around the expected position of the line was adopted for the sources in our Type-2 sample.

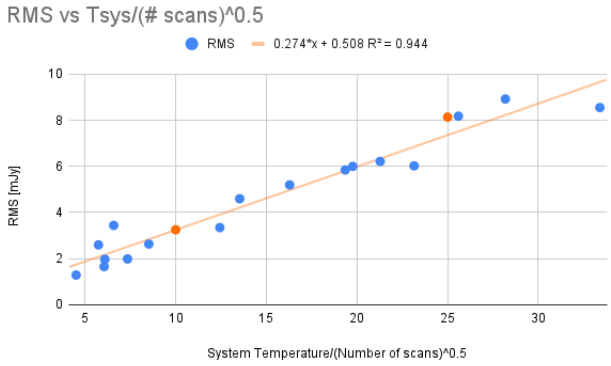

FIG. 3. The RMS on each final spectrum is plotted against $T_{Sys}/\sqrt{n_{scans}}$. This relation is expected to be a positive, linear association, with which the data are consistent. Blue points represent data, orange points represent theoretical calculations, and a line is found to be a good fit to both real and theoretical points.

V. ACKNOWLEDGEMENTS

I would like to thank all members of my summer research team for their parts in this project, with a special thanks to my mentors, Tapasi Ghosh and Chris Salter, for all their support and guidance throughout.

[1] S. J. Curran and S. W. Duchesne, **476**, 3580 (2018), arXiv:1802.05760 [astro-ph.GA].
[2] K. Jones, R. Minchin, C. Salter, and T. Ghosh, *SURVEYING COOL GAS IN HIGH-Z SDSS-III/ BOSS TYPE-2 QUASARS USING HI-ABSORPTION* (GBT Observing Application, 2020).
[3] C. J. Salter, D. J. Saikia, R. Minchin, T. Ghosh, and Y. Chandola, **715**, L117 (2010), arXiv:1004.4006 [astro-ph.CO].

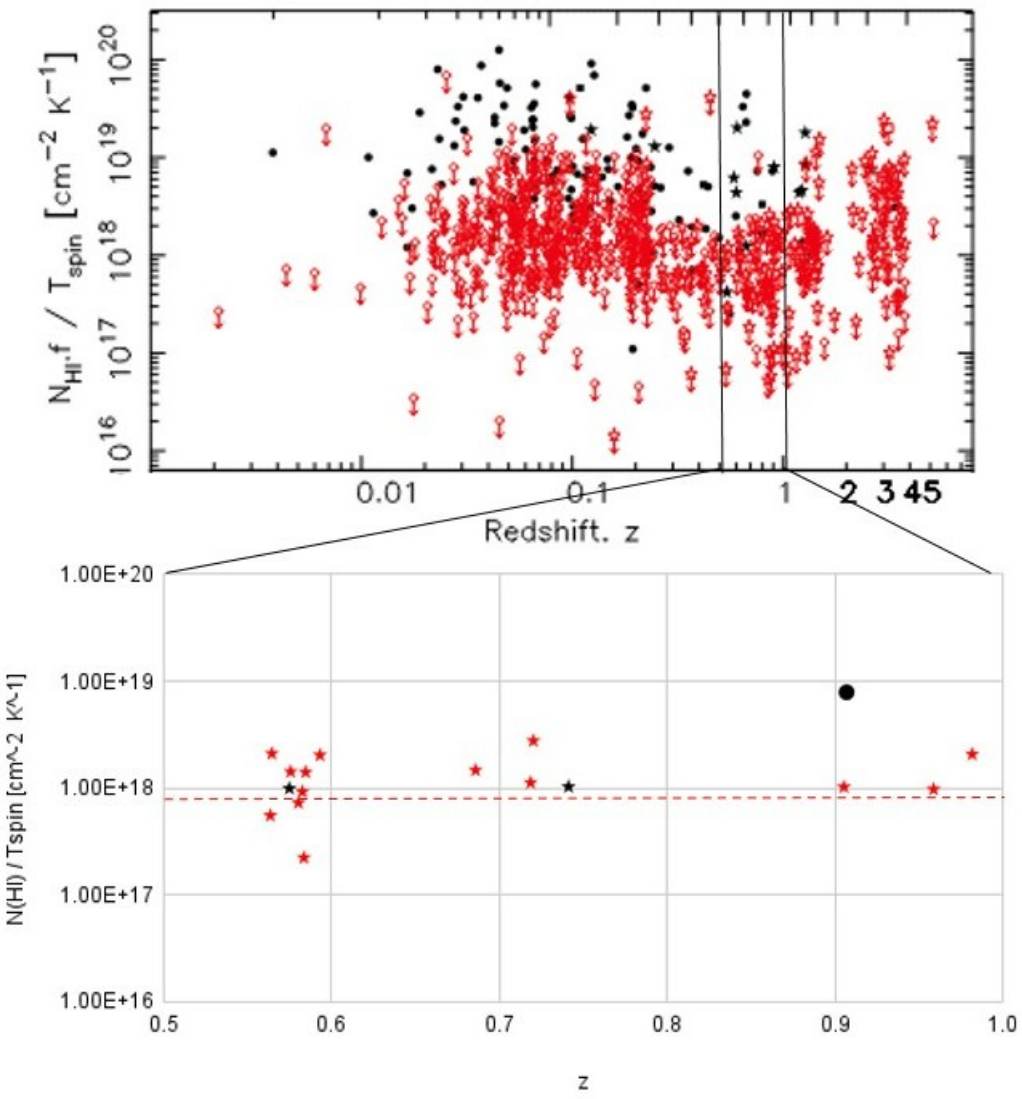

FIG. 4. The top panel is from Curran and Duchesne 2018 [1]. Red points represent the upper limits for HI nondetections while black, solid points represent detections. The authors use stars to indicate quasars and circles to indicate galaxies. The bottom panel plots the sources for this project, where again red points represent nondetection upper limits and the three black points represent the known detection of galaxy CTA21 and this project's two potential detections. The dotted horizontal red line denotes the approximated mean of Curran and Duchesne's points in this redshift range.